JOURNAL OF GEOPHYSICAL RESEARCH, VOL. 105, NO. D3, PAGES 3983–4002, FEBRUARY 16, 2000

Turbulent mixing and the chemical breakdown of isoprene in the atmospheric boundary layer

G. H. L. Verver

Royal Netherlands Meteorological Institute, De Bilt, Netherlands

H. van Dop

Institute for Marine and Atmospheric Research, Utrecht University, Utrecht, Netherlands

A. A. M. Holtslag

Meteorology and Air Quality Section, Wageningen University, Wageningen, Netherlands

Abstract. In this paper we study the effect of turbulence on the oxidation rate of isoprene and its reaction products in the atmospheric boundary layer. We use two models of different complexity: a simple model consisting of two well-mixed layers and a one-dimensional off-line second-order closure model. Both models include an extensive set of chemical reactions to describe the oxidation of isoprene. A 5-day simulation is performed to compare the simple model output with data from the Amazon Boundary Layer Experiment (ABLE-2A). The model is able to represent fairly the basic dynamics and chemistry during this experiment. Subsequently, the simple model provides boundary and initial conditions for a one-dimensional second-order closure model that is used to assess the impact of higher-order chemistry terms on turbulent mixing and chemical transformations. We focus on covariances of NO with (peroxy-)radicals and covariances of OH with stable intermediate products. We find only small effects on the effective reaction rates due to the OH covariances. A significant effect is found of the covariances of NO, inhibiting the effective reaction rates with the peroxy radicals by a maximum of 10% in the afternoon. The inclusion of covariance terms resulted in an increase of radical concentrations, but the NO concentration profiles remained unchanged. Higher-order chemistry terms do have an effect on NO and NO_2 fluxes, which change by 5 to 30% in the middle of the boundary layer. Therefore these terms have to be taken into account when flux-gradient relationships or deposition velocities are derived from observations. The present results indicate that the incorporation of higher-order chemistry terms is not essential for a correct representation of the mean profiles of most stable species involved.

1. Introduction

In the atmosphere, simultaneous mixing and reacting of gases occur. As in a cooking pot, stirring the fluid mixes the contents, effectively bringing the reactants together but also diluting the mixture. Both effects have an impact on the efficiency of the chemical transformations that takes place.

In the atmospheric boundary layer (ABL) the stirring is done by turbulence, generated by friction and buoyancy. The turbulent velocity field working on a concentration gradient will generate concentration fluctuations of scales that range from Kolmogorov's microscale to the scale of the boundary layer height. For an inert gas, the lifetime of the concentration fluctuations will be approximately equal to the dissipation timescale of the turbulent eddies. In general, the gradient of the mean concentration will be large when the mixing process is slow and small when the mixing process is fast. The lifetime of the concentration fluctuations of highly reactive gases will be considerably smaller, and the mean concentration gradient close to the source will be large. Turbulence working on this large gradient will generate fluctuations that are large compared to the local mean concentrations. For reactive gases the conventional gradient diffusion approach to turbulent transport will fail, since the diffusion coefficient will depend on the chemical properties of the transported scalar.

Paper number 1999JD900956.
0148-0227/00/1999JD900956$09.00

Restricting ourselves to bimolecular reactions, the mean transformation rates can significantly change owing to correlated concentration fluctuations. The situation is complicated further by the fact that concentration fluctuations are not only generated by turbulence but also by chemistry itself. To illustrate this, consider a well-mixed boundary layer with a homogeneous concentration of gas i. If a gas j reacting with i is emitted by a point source, gas i will be locally depleted by the chemical reaction. This introduces a concentration fluctuation in a previously homogeneous concentration field of gas i, which will affect the transformation rate of both species.

In this paper we study the higher-order chemistry effects on the fluxes and the effect of correlated concentration fluctuations on a comprehensive chemical scheme that describes the oxidation of isoprene. Isoprene is emitted by vegetation and is one of the most important nonmethane hydrocarbons determining the background tropospheric ozone concentration. It has been suggested [*Davis*, 1992] that the effects of covariance of concentration fluctuations of OH and isoprene may influence its rate of destruction. Our chemistry scheme therefore comprises much more than the simple NO-NO_2-O_3 photochemistry that has been used in most of previous case studies. *Gao and Wesely* [1994] used a similar set of chemical reactions, but their study was limited to a neutral nonentraining boundary layer, in which segregation effects were neglected. In contrast, we explicitly take into account segregation of gases that react. We incorporate the buoyancy term in the flux equation for nonneutral circumstances and allow for entrainment fluxes at the top of the boundary layer. Moreover, this study focuses on a case that is well documented by measurements.

The approach consists of two steps: (1) an integration over several days of a simple two-layer bulk model and (2) 1-hour integrations of a one-dimensional second-order closure model. We compare the results of the simple model with observations. The two-layer model provides a consistent and realistic set of initial and boundary conditions for the second-order closure model. The latter model solves the Reynolds-averaged equations for the mean concentration, turbulent flux, and covariance of concentration and temperature fluctuations as a function of height [*Verver et al.*, 1997]. The chemistry terms of all these equations are taken into account explicitly. To assess the impact of segregation and the chemistry terms in the second-order equations, we compare runs that include these terms with runs in which they are neglected.

In the next section we describe the background of the problem in terms of the Reynolds averaged equations. Section 3 describes the Amazon Boundary-Layer Experiment (ABLE-2A) that we use as a case study. Sections 4 and 5 reflect our two-step approach: the bulk model and the second-order closure model, respectively. We end with a summary and discussion of the results (section 6).

2. Background

The interaction of mixing and chemical transformation described in the introduction can be best illustrated with the Reynolds averaged equations. As an example, we consider only one bimolecular reaction ($i + j \rightarrow$ product). The mean concentration of species i in horizontally homogeneous conditions is given by (no summation over i and j is implied here and hereafter)

$$\frac{\partial C_i}{\partial t} = -\frac{\partial \overline{c_i w}}{\partial z} - k_{ij}(C_i C_j + \overline{c_i c_j}), \tag{1}$$

where C_i and c_i are the mean and fluctuating parts of the instantaneous concentration of species i, respectively, w is the fluctuating part of the vertical velocity and k_{ij} is the reaction constant. The overbar indicate an ensemble average of products of fluctuating quantities. If either species i or j has a chemical lifetime much longer then the timescale of turbulence, $\overline{c_i c_j}$ can usually be neglected. A relevant dimensionless number is the Damköhler number (Da), defined as the ratio of the turbulence timescale and the chemistry timescale [*Danckwerts*, 1952]. However, it was found that $\overline{c_i c_j}$ not only depends on the Damköhler number but also on the flux ratio of the species i and j [*Vilà-Guerau de Arellano and Duynkerke*, 1992]. The importance of $\overline{c_i c_j}$ relative to the mean chemistry term is reflected in the intensity of segregation I_s, defined as

$$I_s \equiv \frac{\overline{c_i c_j}}{C_i C_j}. \tag{2}$$

The lower limit of I_s is -1, when species i and j are fully segregated. When $I_s = 0$ the concentration fluctuations are uncorrelated, as in a well-mixed situation. When I_s is much larger than 0, both gases are concentrated in the same air parcels.

The equation for the covariance $\overline{c_i c_j}$ reads

$$\frac{\partial \overline{c_i c_j}}{\partial t} = -\overline{c_i w}\frac{\partial C_j}{\partial z} - \overline{c_j w}\frac{\partial C_i}{\partial z} - \frac{\partial \overline{c_i c_j w}}{\partial z} - 2\nu_c\overline{\left(\frac{\partial c_i}{\partial x_k}\right)\left(\frac{\partial c_j}{\partial x_k}\right)} + R_{ij}, \tag{3}$$

where ν_c is the molecular diffusivity for gases, and R_{ij} is the chemical term for the bimolecular reaction between i and j, defined as

$$R_{ij} = -k(C_i\overline{c_i c_j} + C_j\overline{c_i c_j} + C_i\overline{c_j^2} + C_j\overline{c_i^2} + \overline{c_i^2 c_j} + \overline{c_i c_j^2}). \tag{4}$$

The first two terms of (3) show that the covariance is generated by the fluxes and gradients of both species. When i and j are transported in the same direction, a positive covariance is generated, since gradients and fluxes have opposite signs. When they are transported

in opposite directions, the first two terms in (3) are negative, and an anticorrelation will develop. The third term describes turbulent transport of covariance and only redistributes $\overline{c_i c_j}$. The fourth term is a sink of covariance due to molecular dissipation.

Equation (4) specifies the chemical production or destruction of covariance R_{ij}. Here we have two effects. The correlation, either positive or negative, of concentration fluctuations are destroyed by chemistry due to the first two terms and will be forced to zero. In patches of air with high concentrations of both i and j (i.e., when they are positively correlated), chemical depletion of both species takes place faster than in patches with low concentrations. Concentration fluctuations and their covariances will therefore decrease. Terms 3 and 4 are always negative, showing that concentration variance of one species may induce a negative covariance due to chemistry. The shape of the triple correlation is unknown, but when we assume symmetric distributions around the mean concentrations, these terms are zero.

The impact of chemical reactions on the applicability of K theory can be illustrated by the equation for the mean flux:

$$\frac{\partial \overline{c_i w}}{\partial t} = -\overline{w^2}\frac{\partial C_i}{\partial z} + \beta \overline{c_i \theta_v} - \frac{\partial \overline{c_i w^2}}{\partial z} - \frac{1}{\rho} c_i \frac{\overline{\partial p}}{\partial z} + R_{wi}, \quad (5)$$

with, for the bimolecular reaction between i and j,

$$R_{wi} = -k_{ij}(C_i \overline{c_j w} + C_j \overline{c_i w} + \overline{c_i c_j w}), \quad (6)$$

where β is g/Θ_{v0}. Θ_{v0} and θ_v are mean and fluctuating parts of the virtual potential temperature. The terms on the right of (5) represent the mean production, the buoyant production, the turbulent transport, the pressure covariance term, and the chemistry term, respectively. The last term is specified in (6) and shows that the turbulent flux now depends on the chemical properties of the reactive scalar itself, as well as on the flux of the gases with which it reacts. It suggests that K, defined as the ratio of the flux and the gradient of the mean concentration, must depend on the reaction rate k_{ij}.

The effects of higher-order chemistry terms, specified above, have been studied by several authors in the past. Chemistry corrections of K theory are proposed based on R_{wi} and similar terms in the equation for $\overline{c_i \theta_v}$ [*Hamba*, 1993; *Verver*, 1994; *Vilà-Guerau de Arellano and Duynkerke*, 1992]. It was shown that for a single bimolecular reaction these corrections are substantial for moderate ($Da \approx 1$) and fast chemistry ($Da > 1$) [*Verver et al.*, 1997]. *Gao and Wesely* [1994] studied a neutral, nonentraining boundary layer assuming $I_s = 0$, incorporating a large number of chemical reactions that describe the photochemical breakdown of isoprene. They found a significant impact on fluxes of NO, NO_2, NO_3, N_2O_5, and OH.

Petersen and Holtslag [1999] derived expressions based on a mass flux scheme for concentration covariances of reactive species for the surface layer and lower mixed layer. Sensitivity runs with this scheme indicated that covariances might have an impact on hydrocarbon and NO_x concentrations.

Schumann [1989] used large-eddy simulations of the convective boundary layer to study segregation effects of two reactive tracers: one released near the surface diffusing upward, and one released near the top diffusing downward. The concentration fluctuations became negatively correlated. He found that the intensity of segregation, I_s, could reach a value as low as -0.7.

Significant effects of I_s on the conversion of NO to NO_2 were found at several hundreds to thousands meters downwind from a point source, depending on the emission strength and Damköhler number [*Georgopoulos and Seinfeld*, 1986; *Karamchandani and Peters*, 1987; *Vilà-Guerau de Arellano et al.*, 1990; *Galmarini et al.*, 1995]. It has been shown that chemistry effects are important to derive deposition velocities of reactive species from observed surface layer concentration profiles. *Fitzjarrald and Lenschow* [1983], *Vilà-Guerau de Arellano and Duynkerke* [1992], *Hamba* [1993], and *Kristensen et al.* [1997] suggested chemistry corrections of the flux-profile relationships for reactive species in the surface layer.

The effects that are found are usually obtained with boundary layer models that incorporate only very simple chemistry and they are not directly verified by experiments, except in the case of dispersion in plumes or in wind tunnels. Higher order chemistry terms will not be taken into account by regional and global chemistry-transport models, unless the possible consequences are assessed.

3. Case Study: The Amazon Boundary-Layer Experiment (ABLE-2A)

In this study we focus on the Amazon Boundary Layer Experiment (ABLE-2A). This field experiment characterized chemistry and dynamics of the dry atmospheric boundary layer over the Amazon Basin during July and August 1985 [*Harriss et al.*, 1988]. The chemical composition of the boundary layer is in this case determined by the emission and chemistry of isoprene, methane, and nitrogen oxides. The BL dynamics as well as the chemical composition have been well documented and provides us with a relevant and realistic case to investigate the impact of higher-order chemistry terms.

During the experiment the emission of isoprene from vegetation exhibits a diurnal cycle with a midday maximum, when solar radiation is largest. A total emission of isoprene of 25,000 $\mu g\ m^{-2}$ per day is estimated by *Zimmerman et al.* [1988]. Figure 1 shows the surface

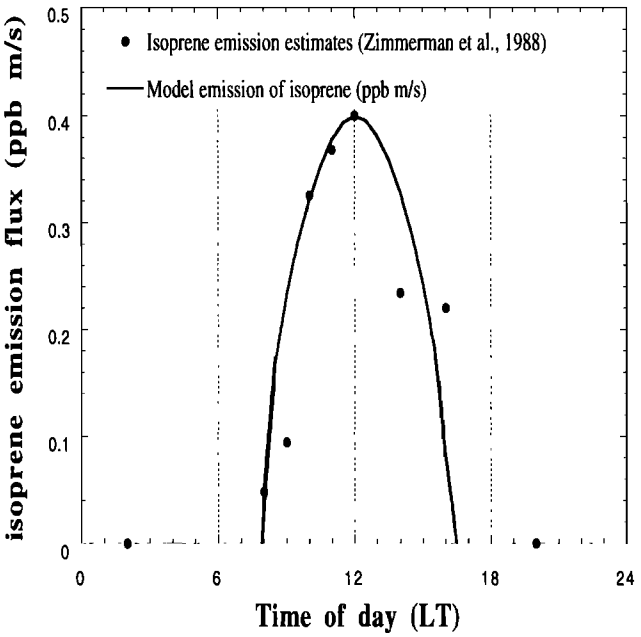

Figure 1. Isoprene emission estimate during ABLE-2A [*Zimmerman et al.*, 1988] and the curve fit used by the two-layer model (1 ppb $ms^{-1} \approx 3\ \mu gm^{-2}s^{-1}$)

flux of isoprene during the day as measured [*Zimmerman et al.*, 1988] and used in our calculations. *Kaplan et al.* [1988] estimated a surface flux of NO of 0.02 ppb $m^{-2}s^{-1}$ during all hours.

The tropical forest is an efficient sink for ozone [*Kaplan et al.*, 1988; *Kirchhoff*, 1988; *Gregory et al.*, 1988]. Deposition velocities that are used in this study are 3 cm s^{-1} for HNO_3, 2.5 cm s^{-1} for O_3 and NO_2, 2 cm s^{-1} for PANs, and 1 cm s^{-1} for peroxides, aldehydes, and ketones. During nighttime we multiply these values by 0.5 to take into account the larger aerodynamic resistance. For isoprene we assume that there is only deposition at night. An apparant deposition velocity of 1 cm s^{-1} is applied, which incorporates a possible nighttime chemical loss within the canopy [*Jacob and Wofsy*, 1988; *Zimmerman et al.*, 1988]. The deposition velocities are similar to values used by *Jacob and Wofsy* [1988] and are partly based on the interpretation of observations during ABLE-2A. However, some values are high compared to deposition velocities given in literature [e.g., *Wesely*, 1989; *Guenter and Hills*, 1998], so they remain a source of uncertainty. The physical characterization of the boundary layer is given by *Martin et al.* [1988].

The oxidation of isoprene consists of a complex chain of reactions that starts with O_3 or OH. During daytime the reaction with OH dominates [*Zimmerman et al.*, 1988], producing an isoprene peroxy radical ($RISOO_2$). This is quickly transformed into stable products methyl vinyl ketone (MVK), metacrolein (MACR), and formaldehyde. MVK and MACR are eventually oxidized to CO and CO_2, consuming OH and transforming NO to NO_2, which leads to photochemical production of O_3. The chemical scheme consists of 71 reactions (Table 1) and 36 chemical species (Table 2). It is based on work of *Atkinson et al.* [1982] and *Trainer et al.* [1987] and was applied by *Gao et al.* [1991] and *Gao and Wesely* [1994]. Photolysis rates are calculated with an algorithm described by *Kuhn et al.* [1998]. Reactions and chemical components are listed in the appendix. A simplified picture that summarizes the chemical scheme is given in Figure 2. This set of chemical reactions is used consistently throughout this study.

4. Bulk Approach

4.1. Concepts

The chemical composition of the boundary layer over the tropical forest is described by a two-layer bulk model, which incorporates the whole boundary layer (BL) as a well-mixed box with entrainment fluxes, surface fluxes, and a prescribed boundary layer evolution. The equation for the layer-average concentration (indicated by angle brackets) of species i in the BL is then (see equation (1)):

$$\frac{\partial < C_i >_{BL}}{\partial t} = \frac{F_s(t) - F_e(t)}{h(t)} + \text{Chemistry}(t), \quad (7)$$

where F_s is the surface flux, F_e is the entrainment flux, and h is the BL height that varies during the day. We use a schematic representation of the boundary layer evolution as depicted in Figure 3, which is based on radio soundings made on days during ABLE-2A that were not significantly disturbed by clouds or precipitation [*Martin et al.*, 1988].

We use for the maximum and minimum boundary layer height 1500 and 300 m, respectively. A linear growth of the boundary layer is defined during the morning hours between 0800 (t_1) and 1300 (t_2) LT. At 1800 LT a fraction of the mass of each species is captured in the reservoir layer (RL), where is remains decoupled from the surface until the next morning when it is transported into the BL by entrainment. The entrainment flux between times t_1 and t_2 of species i is calculated by (see, e.g., *Nappo and van Dop*, 1994)

$$F_e = \frac{dh}{dt}(< C_i >_{BL} - < C_i >_{RL}). \quad (8)$$

Initial concentrations for the two-layer model are taken from *Jacob and Wofsy* [1988], but after 3 days, model results are not very sensitive to the initial values that are chosen, except for the concentration of CO and CH_4 (150 and 1700 ppb, respectively). The latter two are kept constant and uniform in the model throughout the simulations. Chemical transformations in the BL and RL are calculated using the mean concentrations in these layers.

Table 1. The Chemical Scheme

	Reaction	Reaction Rate	Reference
R1	$O^3P + O_2 + M \rightarrow O_3 + M$	0.733E5	1
R2	$O_3 + NO \rightarrow NO_2 + O_2$	$(17/T)\exp(-1450/T)$	1
R3	$O^3P + NO_2 \rightarrow NO + O_2$	0.22	2
R4	$O_3 + NO_2 \rightarrow NO_3 + O_2$	$(0.88/T)\exp(-2450/T)$	2
R5	$NO_3 + NO \rightarrow 2NO_2$	0.22	1
R6	$NO_3 + NO_2 \rightarrow N_2O_5$	$(520/T)\exp(-1100/T)$	1
R7	$N_2O_5 + M \rightarrow NO_3 + NO_2 + M$	$6.3E14\exp(-10970/T)$	1
R8	$OH + NO_2 \rightarrow HNO_3$	$2.5E4/T^2$	1
R10	$HO_2 + NO \rightarrow NO_2 + OH$	$62/T$	1
R13	$N_2O_5 + H_2O \rightarrow 2HNO_3$	$[H_2O]2.2E\text{-}8/T$	1
R14	$OH + HNO_3 \rightarrow NO_3$	$2.4E\text{-}4\exp(778/T)$	3
R15	$HO_2 + HO_2 \rightarrow H_2O_2 + O_2$	0.06	1
R16	$CO + O_2 + OH \rightarrow CO_2 + HO_2$	0.007	1
R17	$NO_2 + h\nu \rightarrow NO + O^3P$	variable	4
R18	$H_2O_2 + h\nu \rightarrow 2OH$	variable	4
R20	$O_3 + h\nu \rightarrow O_2 + O^1D$	variable	4
R21	$O_3 + h\nu \rightarrow O_2 + O^3P$	variable	4
R22	$HCHO + h\nu \rightarrow 2HO_2 + CO$	variable	4
R23	$HCHO + h\nu \rightarrow H_2 + CO$	variable	4
R24	$O^1D + H_2O \rightarrow 2OH$	$[H_2O]5.7$	1,3
R25	$O^1D + M \rightarrow O^3P + M$	0.72E9	1,3
R26	$HCHO + OH \rightarrow HO_2 + CO$	0.35	1,3
R28	$HNO_3 + h\nu \rightarrow NO_2 + OH$	variable	4
R29	$NO_3 + h\nu \rightarrow NO_2 + O^3P$	variable	4
R30	$N_2O_5 + h\nu \rightarrow NO_2 + NO_3$	variable	4
R31	$NO_2 + HO_2 \rightarrow HNO_4$	0.027	2
R32	$HNO_4 + h\nu \rightarrow HO_2 + NO_2$	variable	4
-	$HNO_4 + M \rightarrow HO_2 + NO_2$	$(4.6E\text{-}16/T)\exp(10870/T)$	2,3
R33	$O_3 + OH \rightarrow HO_2$	$(12/T)\exp(-940/T)$	3
R34	$O_3 + HO_2 \rightarrow OH$	$(9.8E\text{-}2/T)\exp(-580/T)$	3
R35	$CH_4 + OH \rightarrow CH_3O_2 + H_2O$	$(17/T)\exp(-1710/T)$	1,3
R36	$CH_4 + O^1D \rightarrow CH_3O_2 + OH$	$9.8E2/T$	1,3
R37	$CH_3O_2 + NO \rightarrow HCHO + HO_2 + NO_2$	$(29/T)\exp(180/T)$	1,3
R38a	$CH_3O_2 + HO_2 \rightarrow CH_3OOH + O_2$	$(5.4E\text{-}1/T)\exp(1300/T)$	1,3
R38b	$CH_2O_2 + NO \rightarrow CH_2O + NO_2$	0.1785	3
R38c	$CH_2O_2 + NO_2 \rightarrow CH_2O + NO_3$	0.1785	3
R38d	$CH_2O_2 + H_2O \rightarrow$ products	$[H_2O]8.4E\text{-}8$	3
R39	$CH_3OOH + OH \rightarrow 0.56CH_3O_2 + 0.44HCHO + 0.44OH + 0.44CO + H_2O$	$70/T$	3
R40	$CH_3OOH + h\nu \rightarrow HCHO + OH + HO_2$	variable	4
R41	$CH_3CHO + h\nu \rightarrow CH_3O_2 + HO_2 + CO$	variable	4
R42	$OH + CH_3CHO \rightarrow CH_3CO_3$	$(50/T)\exp(250/T)$	1,3
R43	$CH_3CO_3 + NO_2 \rightarrow PAN$	$35/T$	1
R44	$PAN \rightarrow CH_3CO_3 + NO_2$	$1.6E16\exp(-13253/T)$	3
R45	$CH_3CO_3 + NO \rightarrow NO_2 + CH_3O_2$	$51.7/T$	1
R51	$OH + \text{isoprene} \rightarrow RISOO_2$	$(170/T)\exp(409/T)$	1
R52	$RISOO_2 + NO \rightarrow 0.9NO_2 + 0.9HO_2 + 0.9HCHO + 0.45MVK + 0.45MACR + 0.1\text{nitrates}$	$(31/T)\exp(180/T)$	1
R53	$O_3 + \text{isoprene} \rightarrow 0.5HCHO + 0.2MVK + 0.3MACR + 0.2CH_2O_2 + 0.05HO_2 + 0.2CO + 0.2MVKOO + 0.3MAOO$	$(0.051/T)\exp(-1900/T)$	1
R54	$MVKOO + NO \rightarrow MVK + NO_2$	$(31/T)\exp(180/T)$	1
R55	$MVKOO + NO_2 \rightarrow MVK + NO_3$	$5.1/T$	1
R56	$MVKOO + H_2O \rightarrow$ stable products	$[H_2O]2.5E\text{-}5/T$	1
R57	$MAOO + NO \rightarrow MACR + NO_2$	$(31/T)\exp(180/T)$	1
R58	$MAOO + NO_2 \rightarrow MACR + NO_3$	$5.1/T$	1
R59	$MAOO + H_2O \rightarrow$ stable products	$[H_2O]2.5E\text{-}5$	1
R60	$OH + MVK \rightarrow MVKOO$	$(25/T)\exp(500/T)$	1
R61	$NO + MVKOO \rightarrow 0.9NO_2 + 0.6CH_3COO_2 + 0.6HAC + 0.3HO_2 + 0.3CH_2O + 0.3MGLY$	$(31/T)\exp(180/T)$	1
R62	$OH + HAC \rightarrow HACO_2$	$110/T$	1
R63	$HACO_2 + NO_2 \rightarrow HPAN$	$34/T$	1,3
R64	$HPAN \rightarrow HACO_2 + NO_2$	$1.6E16\exp(-13253/T)$	2
R65	$HACO_2 + NO \rightarrow HO_2 + CH_2O + NO_2$	$(31/T)\exp(180/T)$	3

Table 1. (continued)

	Reaction	Reaction Rate	Reference
R66	$OH + MGLY \rightarrow CH_3COO_2 + CO + H_2O$	$120/T$	1,3
R67	$OH + MACR \rightarrow MAOO_2$	$73/T$	1,3
R68	$MAOO_2 + 3NO \rightarrow 3NO_2 + HO_2 + MGLY$	$(31/T)\exp(180/T)$ ($ppb^{-1}s^{-1}$)	1,3
R69	$MAOO_2 + NO_2 \rightarrow MPAN$	$35/T$	1,3
R70	$MPAN \rightarrow MAOO_2 + NO_2$	$1.6E16\exp(-13253/T)$	2
R71	$OH + MACR \rightarrow MRO_2$	$(29/T)\exp(500/T)$	1,3
R72	$MRO_2 + NO \rightarrow 0.9NO_2 + 0.9HO_2 + 0.9CH_2O + 0.9MGLY + 0.1$ nitrates	$(31/T)\exp(180/T)$	1,3
R73	$O_3 + MVK \rightarrow 0.5CH_2O + 0.5MGLY + 0.2CH_2O_2 + 0.2CO + 0.2HO_2 + 0.2MCRIG + 0.15CH_3CHO + 0.15CH_3COO_2$	$(2.9E2/T)\exp(-2000/T)$	1,3
R74	$O_3 + MACR \rightarrow 0.5HCHO + 0.5MGLY + 0.2CH_2OO + 0.35CO + 0.21HO_2 + 0.2MCRIG + 0.15CH_3O_2$ + stable products	$(3.7E\text{-}2/T)\exp(2500/T)$	1,3
R75	$MCRIG + NO \rightarrow MGLY + NO_2$	$(31/T)\exp(180/T)$	1,3
R76	$MCRIG + NO_2 \rightarrow MGLY + NO_3$	$5.1/T$	1,3
R77	$MCRIG + H_2O \rightarrow$ stable product	$[H_2O]2.5E\text{-}5/T$	1,3
R78	$HAC + h\nu \rightarrow HCHO + 2HO_2$	variable	4
R79	$MGLY + h\nu \rightarrow CH_3CO_3 + HO_2 + CO$	variable	4

Reaction rates in s^{-1} or $ppb^{-1}s^{-1}$ for unimolecular and bimolecular reactions, respectively. Concentrations of O_2 and M are incorporated in the reaction rates (e.g., rates of reactions R1 and R7 are in $ppb^{-1}s^{-1}$). $[H_2O]$ is in ppb and T in Kelvin. Reference numbers: 1, *Gao et al.* [1991] and *Gao and Wesely* [1994], 2, *Calvert and Stockwell* [1983], 3, *Trainer et al.* [1987], 4, *Kuhn et al.* [1998]. Read 0.733E5 as 0.733×10^5.

Table 2. Species

Species	Remarks
Oxygen	
O^3P and O^1D	not transported
O_3	
Nitrogen	
NO, NO_2, NO_3, N_2O_5	
HNO_2, HNO_3, HNO_4	
Isoprene and Intermediate Prod.	
Isoprene	$CH_2=C(CH_3)CH=CH_2$
MVK (methyl vinyl ketone)	$CH_3COCH=CH_2$
MACR (methacrolein)	$CH_2=C(CH_3)CHO$
HAC (hydroxyacetaldehyde)	$HOCH_2CHO$
MGLY (methylglyoxal)	CH_3COCHO
HCHO (formaldehyde)	
CH_3CHO (acetaldehyde)	
Peroxyacetyl Nitrates (PANs)	
PAN	$CH_3CO_3NO_2$
MPAN	$CH_2=C(CH_3)CO_3NO_2$
HPAN	$OHCH_2CO_3NO_2$
Peroxides	
CH_3OOH and H_2O_2	
Peroxy Radicals (RO_2)	
$RISOO_2$	isoprene RO_2
MRO_2	MACR RO_2
$MAOO_2$	$CH_2=C(CH_3)C(O)OO$
$HACO_2$	$OHCH_2C(O)OO$
CH_3CO_3 and CH_3O_2	
Criegee Biradicals	
MVKOO	$CH_2=CHC(OO)CCH_3$
MAOO	$CH_2=C(CH_3)CHOO$
MCRIG	$CH_3COCHOO$
CH_2O_2	
Long-lived Species	
CH_4 and CO	kept constant in time

4.2. Results

Figure 4 depicts the BL concentration versus time obtained from the two-layer model during the fifth day of the simulation. The diurnal variation is a result of boundary layer dynamics, emission, chemistry, and deposition. The last 3 days of the simulation (day 3 to 5) show a similar course of concentration levels of all species.

4.2.1. Isoprene and OH. During nighttime the emission of isoprene and BL dynamics are unimportant for the isoprene concentration. The main reason for the rapid decrease of isoprene in the shallow BL at night is deposition, which accounts for more than 70% of the total loss. It was suggested by *Zimmerman et al.* [1988] that the reaction with the NO_3 radical could be a significant chemical sink of isoprene during nighttime. However, when this reaction was added to our chemistry scheme, using a reaction rate given in *Carter* [1996], we found only a very minor effect, due to the low NO_3 concentration. In the reservoir layer the decrease of isoprene during the night is less than in the boundary layer (see Figure 5) and caused mainly by the reaction with ozone.

The model produces a peak OH concentration in the morning hours which is caused by the combined effect of the diurnal cycles of photolysis rates, BL height and isoprene emission. Just before the BL starts to grow, the increasing solar radiation, and the low level of isoprene at this time allows for a rapid growth of OH. In the model, there is an abrupt start at 0800 LT of both the surface emission of isoprene and the downward entrainment of isoprene and its stable reaction products.

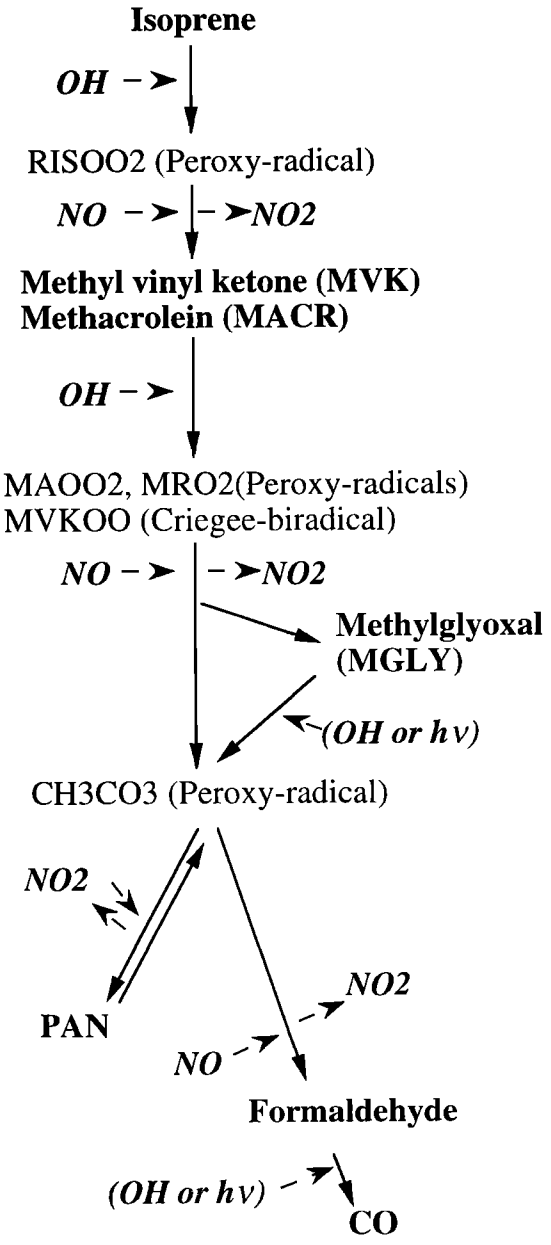

Figure 2. Schematic overview of the chemical breakdown of isoprene.

Since the boundary layer is still shallow at this time of day, concentrations of isoprene, MVK, and MACR increase rapidly, leading to a decreasing OH concentration after 0900 LT. In the work of *Zimmerman et al.* [1988], OH concentrations are given which are based on O_3, isoprene, NO, water vapor, temperature, and radiation observations. The values in the afternoon compare very well with our bulk model results. However, the strong maximum concentration in the morning produced by the model is not confirmed by the derived values. It must, however, be noted that there is a large scatter in the values calculated from the morning observations.

The reaction of isoprene with OH is by far the largest chemical sink for both species during daytime. The reaction peaks around 0900 LT, when both OH and isoprene are abundantly available. The concentration difference between the RL and the BL determines the sign of the entrainment flux (equation (8)). From 0800 to 0900 LT the downward entrainment flux contributes to the BL concentration of isoprene. From 0900 to 1300 LT the entrainment flux is upward, thus diluting the BL with air from the reservoir layer containing much less isoprene. However, there still remains an increase of concentration due to the emission of isoprene by vegetation in this part of the day. The largest increase of isoprene concentration is just after 1300 LT when the BL stopped growing and the emission is close to its maximum daytime value (Figure 1). The maximum value is reached in the afternoon, as was also observed by *Zimmerman et al.* [1988], although the model underestimates BL concentrations by roughly 1 ppb during daytime (Figure 5). From 1600 to 1800 LT, chemical destruction of isoprene dominates over the emission, which causes a fast decrease of the BL concentration. After 1800 LT, there is no emission and deposition is the main sink of isoprene. Nighttime concentrations agree closely with observations (Figure 5).

4.2.2. Nitrogen oxides and ozone. NO_x builds up during the night, due to the continuous emission of NO from the soil into the shallow nighttime boundary layer. Concentrations increase more rapidly in the early morning, due to the photolysis of NO_2 and the lower deposition velocities of NO, which was also found by *Jacob and Wofsy* [1988]. Concentrations of NO_x above the BL are lower, so that entrainment dilutes BL concentrations of NO_x. The peak concentration of OH in the morning results in a sink of NO_x due to the formation of HNO_3. However, during daytime the formation of PAN is the dominant chemical sink.

Concentrations of ozone in the BL and RL are plotted in Figure 5. They closely agree with the BL observations during ABLE-2A [*Gregory et al.*, 1988]. The sharp increase of BL ozone concentration in the morning is caused by entrainment from the RL. The values in the RL remain high throughout the day since this layer is formed at the end of the day, when BL ozone concentrations are still high, and the main sink, deposition, is absent in this layer.

4.2.3. PANs, MVK, and MACR. The continuous decrease of PANs during night is due to dry deposition. The rapid increase in the morning hours is caused by the downward entrainment flux into the shallow nighttime BL. Later in the day, dry deposition and chemical production are more or less balanced. In the late afternoon for some time the thermal dissociation of PAN is larger than the chemical production, increasing NO_2 and decreasing concentration of PAN.

The intermediate products of the breakdown of isoprene, methacrolein (MACR) and methyl vinyl keton (MVK) show a strong diurnal cycle. Early morning is dominated by an influx from above the BL, which causes the sharp rise of concentration, damped a little by chemical destruction through the reaction with OH which is at its maximum concentration during these

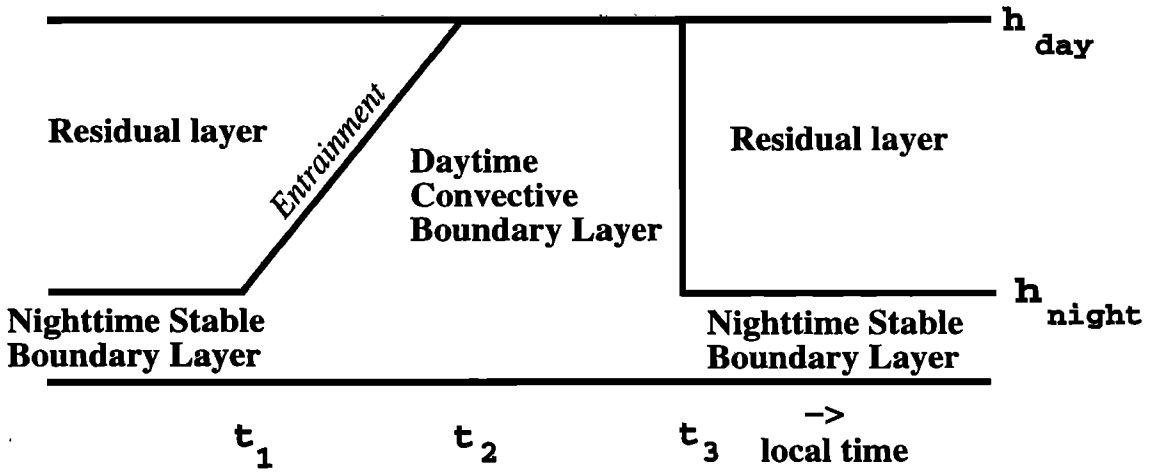

Figure 3. Prescribed boundary layer evolution during the day for the two-layer model.

hours. In the reservoir layer the concentrations of MVK and MACR decrease owing to chemical destruction in combination with the absence of an isoprene source. Roughly 2 hours before the boundary layer reaches its maximum depth, the concentrations in the boundary layer exceed the concentrations in the reservoir layer. This leads to an upward entrainment flux for both species and a slower increase of boundary layer concentrations just before 1300 LT. The discontinuity at 1300 LT is caused by putting the entrainment flux to zero at this time. The continuous builtup of isoprene then causes the concentration maximum in the after-

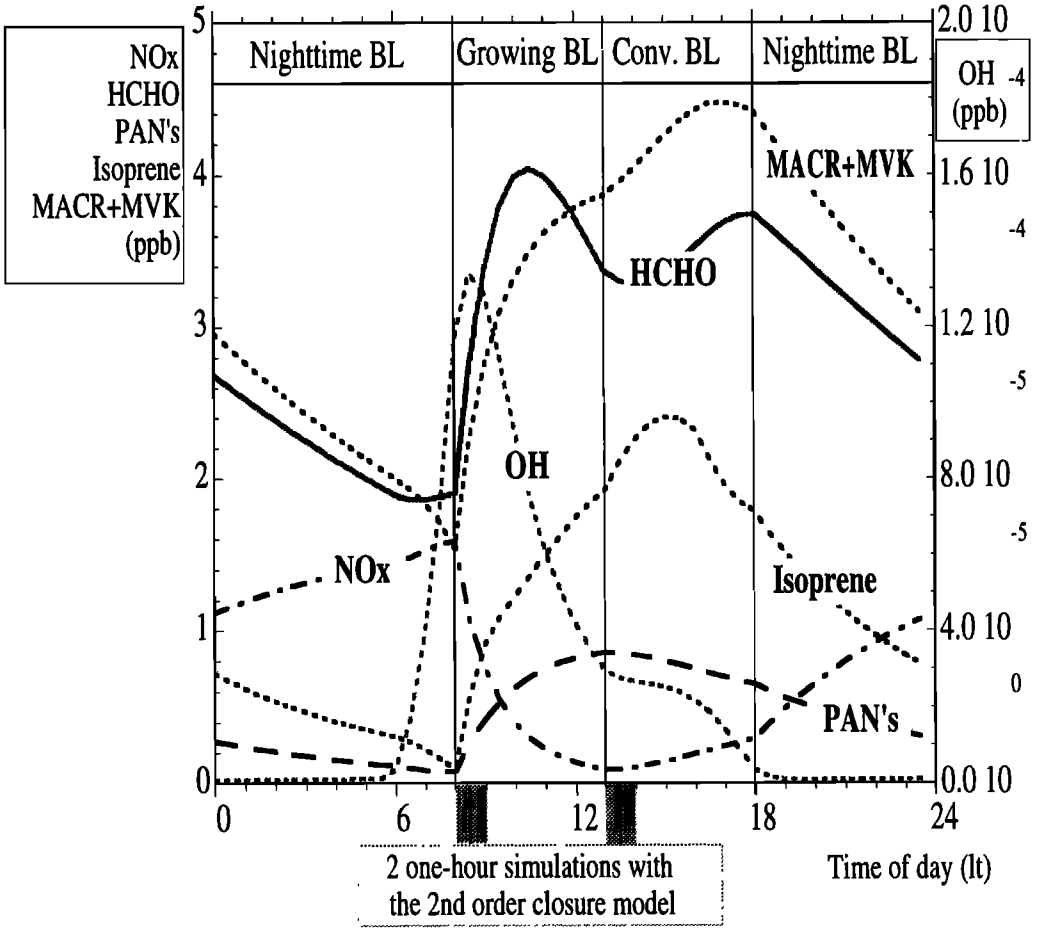

Figure 4. Boundary layer concentrations of NO, NO_2, isoprene, formaldehyde, PANs, OH and the sum of MVK and MACR, during day 5 of the ABLE-2A simulation with the two-layer model.

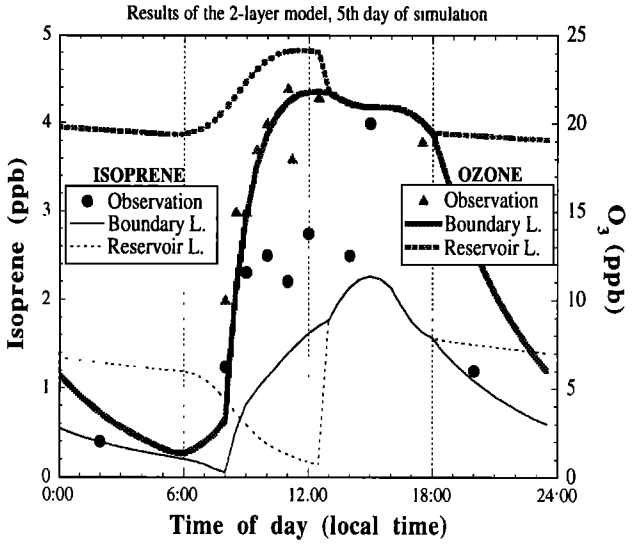

Figure 5. Observed and modeled concentrations of O_3 and isoprene during ABLE-2A. The O_3 observations are boundary layer averages calculated by *Jacob and Wofsy* [1988], based on a number of profiles from *Gregory et al.* [1988]. The observed isoprene concentrations are median mixed-layer values taken from *Jacob and Wofsy* [1988], based on observations of *Zimmerman et al.* [1988]. Model values are taken from day 5 of the simulation with the two-layer model.

noon. Both MACR and MVK are effectively removed by deposition that is assumed to occur at night.

The simple model with two layers is able to represent the basic features of boundary-layer dynamics during one day. The diurnal variation of isoprene, O_3, NO_x, and PAN is in reasonable agreement with observations and previous model studies [*Zimmerman et al.*, 1988; *Gregory et al.*, 1988; *Jacob and Wofsy*, 1988].

5. Second-Order Closure Approach

5.1. Concepts

The turbulent transport and chemical transformations are studied in more detail with a one-dimensional, second-order closure boundary layer model. We only give a brief outline; the full description is given by *Verver et al.* [1997].

The model solves the equations for scalars i in horizontally homogeneous conditions:

$$\frac{\partial C_i}{\partial t} = -\frac{\partial \overline{c_i w}}{\partial z} + R_i, \tag{9}$$

where R_i represents chemical production or destruction of the reactive species i. The model contains budgets for the second moments $\overline{c_i c_j}$, $\overline{c_i w}$, and $\overline{c_i \theta_v}$, all incorporating chemical terms that will be specified later on. Furthermore, the model uses diagnostic equations expressing third moments of concentration ($\overline{c_i c_j c_k}$, $\overline{c_i c_j w}$, $\overline{c_i w^2}$, and $\overline{c_i w \theta_v}$) in terms of second moments and their vertical derivatives.

We prescribe the profiles of the physical quantities that characterize the boundary layer and determine the turbulent transport of scalars (i.e., profiles of $\overline{w^2}$, Θ, $\overline{w\theta}$, $\overline{\theta^2}$ and the length scale l). These profiles are constructed using the convective velocity scale ($w_* \equiv [(g/\Theta_v)h\overline{w\theta_v}]^{1/3}$) and the friction velocity (u_*) that represent the local situation at a specific time. These profiles are independent of the small mixing ratios of trace gases and are kept constant during the 1-hour simulations. Boundary and initial conditions are taken from the two-layer model described in the previous section. The initial profiles are vertically uniform.

In the second-order closure model we explicitly take into account the influence of chemistry on the turbulent flux, covariance of concentration and covariance of concentration and temperature. Explicit chemical terms are neglected in the diagnostic expressions for the third-order quantities. However, since these are expressed in terms of second-order quantities and their vertical derivatives, there is an implicit chemical impact through these terms that is not neglected.

The generic form of the chemistry term R_{wi} in the equation for the turbulent flux of species i is [*Vilà-Guerau de Arellano and Lelieveld*, 1998]

$$R_{wi} = \sum_{m=1}^{N} k_{im}\overline{c_m w} + \sum_{m=1}^{N}\sum_{n=1}^{m} k_{imn}(C_m\overline{w c_n} + C_n\overline{w c_m} + \overline{c_m c_n w}), \tag{10}$$

where k_{im} is the reaction rate for a unimolecular reaction of species m, and k_{imn} is the bimolecular reaction rate of species m and n, both forming or destroying species i. In nonneutral situations, there is a buoyancy term in the flux equation; the impact of chemistry on this term is given by

$$R_{i\theta} = \sum_{m=1}^{N} k_{im}\overline{c_m \theta_v} + \sum_{m=1}^{N}\sum_{n=1}^{m} k_{imn}(C_m\overline{\theta_v c_n} + C_n\overline{\theta_v c_m} + \overline{c_m c_n \theta_v}). \tag{11}$$

The chemistry influence on the covariance and variance of concentration fluctuations is given by

$$R_{ij} = \sum_{m=1}^{N} k_{im}\overline{c_j c_m} + \sum_{m=1}^{N} k_{jm}\overline{c_i c_m} + \sum_{m=1}^{N}\sum_{n=1}^{m} k_{inm}(C_m\overline{c_j c_n} + C_n\overline{c_j c_m} + \overline{c_j c_m c_n}) + \sum_{m=1}^{N}\sum_{n=1}^{m} k_{jnm}(C_m\overline{c_i c_n} + C_n\overline{c_i c_m} + \overline{c_i c_m c_n}). \tag{12}$$

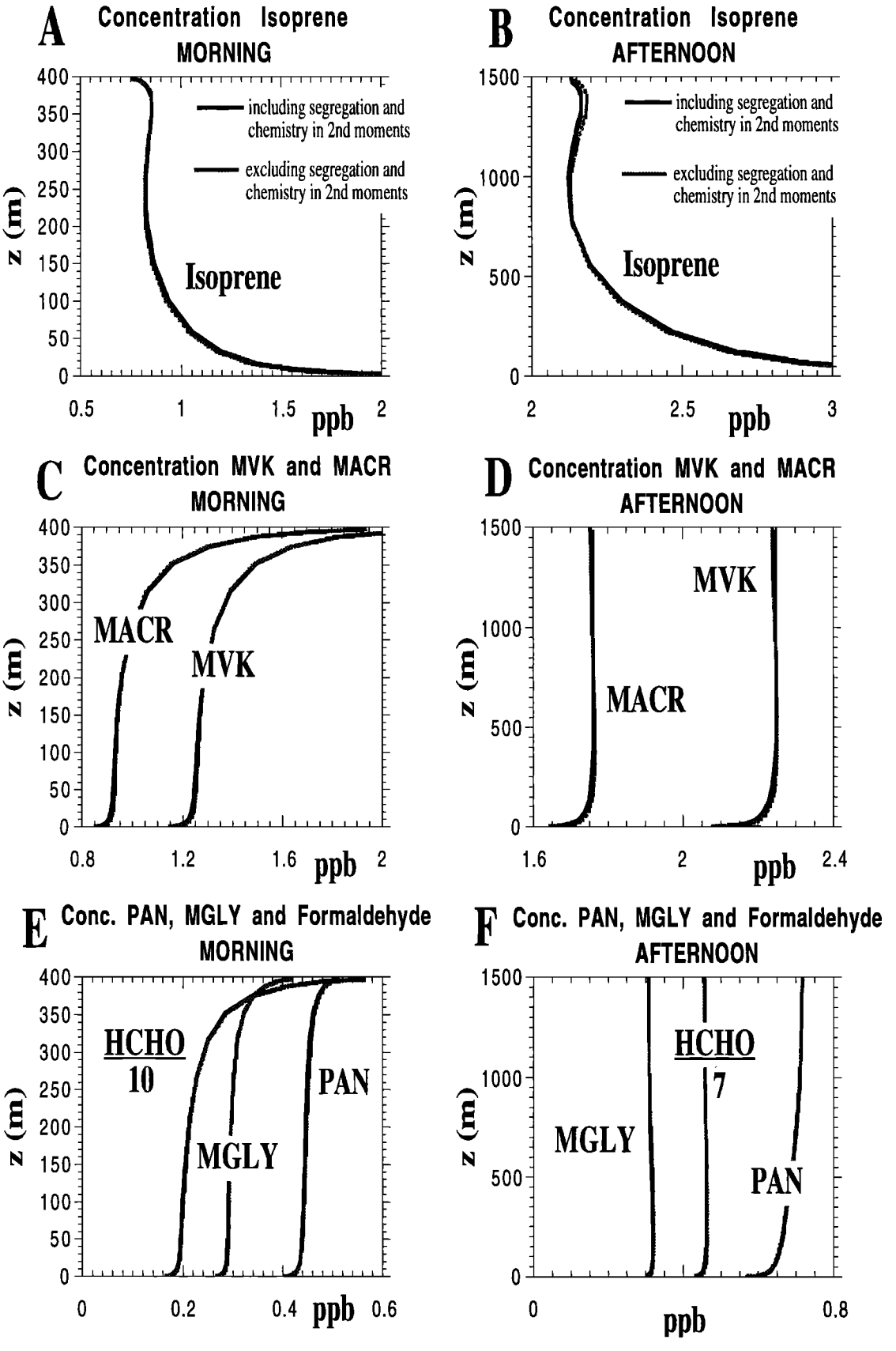

Figure 6. Mean concentration profiles in the (left) morning and (right) afternoon of several stable species. Results of runs that included higher-order chemistry terms are plotted in black; grey lines refer to runs where these terms are neglected.

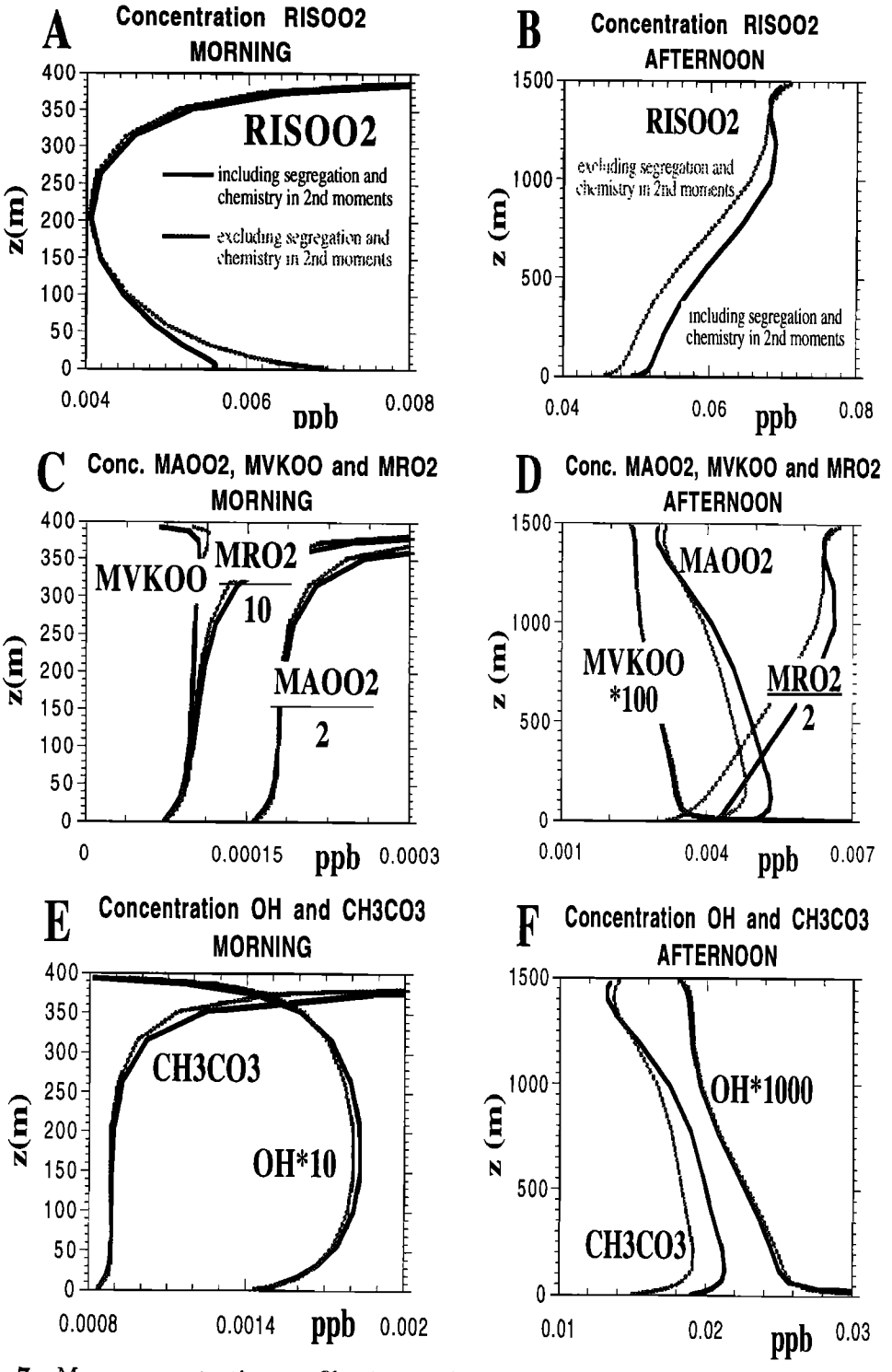

Figure 7. Mean concentration profiles in the (left) morning and (right) afternoon of several short-living radicals. Including (black) and excluding (grey) higher-order chemistry terms.

The chemistry terms, (10), (11), and (12)), introduce a large number of covariances and triple products of fluctuations of concentration, temperature, and vertical velocity. Although they are all calculated, it is clear that in the chemical scheme that is used, only a small subset of these are relevant for the fluxes and covariances. We will focus on these terms.

We initialize the one-dimensional model with results from the two-layer model. Initial values are obtained for the fifth day at 0800 LT and 1300 LT, as indicated by the arrows in Figure 4. The one-dimensional second-order closure model is run for 1 hour to obtain quasi-stationary profiles for the relatively long-lived species, such as ozone and isoprene. (The largest turbulence

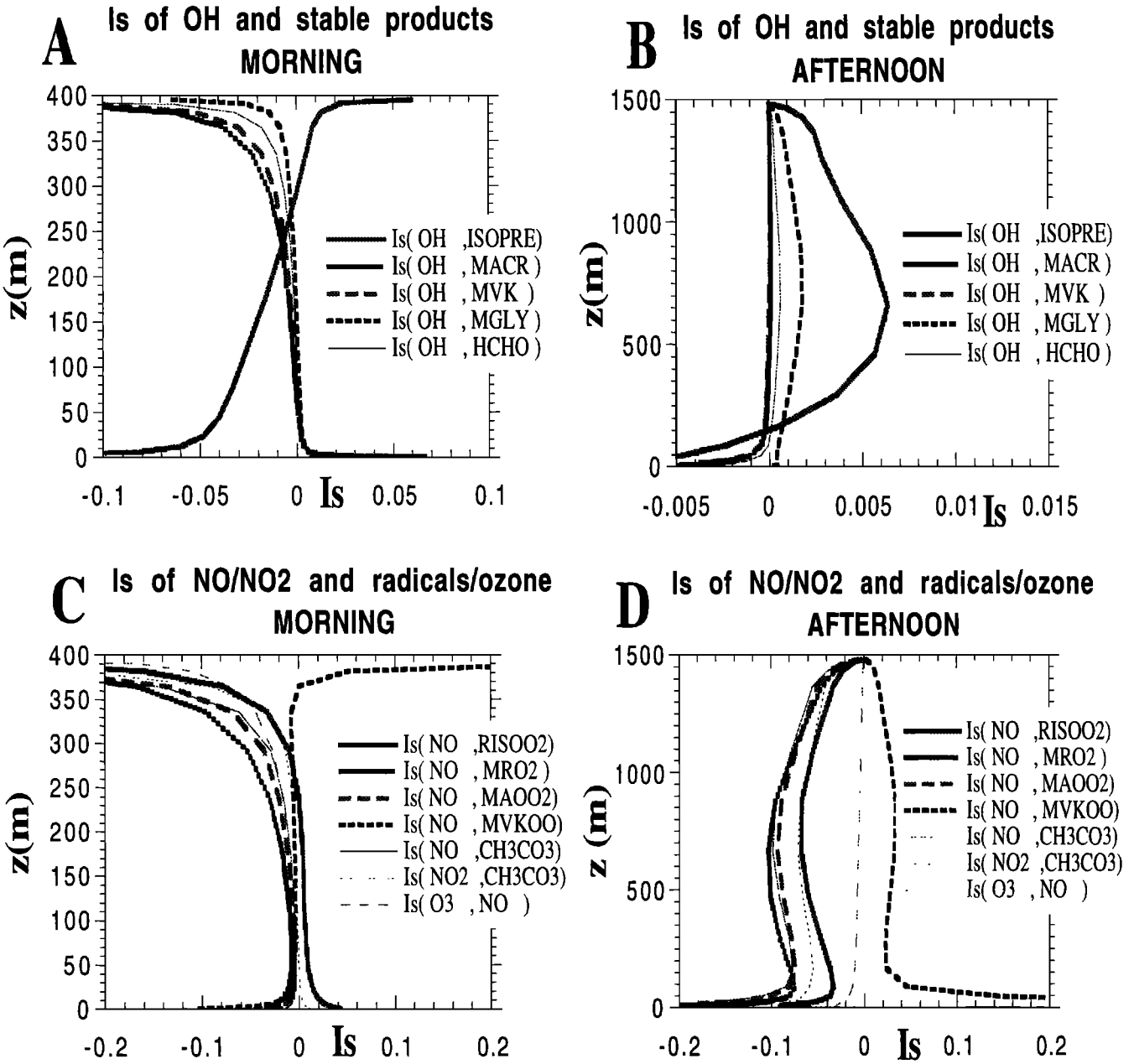

Figure 8. Intensity of segregation $I_s \equiv \overline{c_i c_j}/(C_i C_j)$ for OH and stable products in the (a) morning and (b) afternoon, and for NO and radicals or O_3 in the (c) morning and (d) afternoon.

timescale ($\approx h/w_*$) is 450 and 833 s for the morning and afternoon case, respectively. Therefore after 1 hour quasi-steady state is reached for long-lived species, with nearly linear flux profiles.) Parameters characterizing the convective boundary layer between 0800 and 0900 LT are $w_* = 0.88$ ms^{-1}, $h = 400$m, and between 1300 and 1400 LT $w_* = 1.8$ ms^{-1}, $h = 1500$ m [*Martin et al.*, 1988]. In the 1-D model these values are kept constant throughout the one hour simulation. Deposition velocities, photodissociation constants, and emissions are given the same values as in the two-layer model for the two selected hours. The concentrations of CO and CH_4 (150 and 1700 ppb, respectively) are vertically uniform and kept constant in time.

Between the two cases, early morning from 0800 to 0900 LT and afternoon from 1300 to 1400 LT, there are clear differences with respect to the chemistry and turbulent transport that take place (see Figure 4). In the morning the concentrations are highly nonstationary due to the large entrainment fluxes into the shallow but rapidly growing boundary layer. In contrast, there is no entrainment in the afternoon simulation, and the boundary layer is at its maximum height, so that surface fluxes have only a relatively small effect on the mean concentrations. Isoprene emission, however, is approximately at its maximum daytime value at 1300 LT, causing increasing concentrations of isoprene, MACR and MVK, and subsequent decreasing OH concentra-

tion. During the morning hour simulation OH as well as NO_x are at their highest level and rapidly decrease to the much lower concentrations in the afternoon.

5.2. Results

Concentration, flux, and segregation profiles obtained from the 1-D second-order closure model are presented in Figures 6 to 11, and are discussed in sections 5.2.2 and 5.2.3. All profiles in these figures are snapshots of the model variables taken after one hour of simulation. Quasi-steady state is reached after this time, as indicated by the linear flux profiles of isoprene (Figure 9). We start in the next section with an overview and discussion of timescales of chemistry obtained by the second-order closure model.

5.2.1. Chemistry timescales. To put some order in the large number of gases, we define two Damköhler numbers for each species. The first one is based on the chemistry terms in the equation for the mean concentration. Many gases, especially the radicals, are dominated by both fast production and fast destruction reactions that nearly balance. In order to be able to distinguish between highly reactive species that are near chemical equilibrium and species with low reaction rates, we define a concentration Damköhler number Da_c by

$$Da_c \equiv \max(P_i, -D_i) < C_i >_{BL}^{-1} h/w_*, \qquad (13)$$

where P_i and D_i are the boundary-layer averaged production and destruction of tracer i, respectively. A second Damköhler number is defined using the chemistry terms of the flux equation for species i, specified in (10), averaged over the boundary layer:

$$Da_f \equiv < R_{wi} >_{BL} < \overline{c_i w} >_{BL}^{-1} h/w_*. \qquad (14)$$

Both Da_c and Da_f are calculated for each species and are plotted in Figure 12. Note that we have taken into account the higher-order chemistry terms given in 5.1 and that these numbers are boundary layer averages. Near the surface and top of the boundary layer the local Damköhler numbers may be significantly different since the local turbulence timescale as well as local concentrations change rapidly close to these boundaries.

Species with high Da_c ($\gtrsim 5$) are highly reactive, and if their concentrations change in time, this is mainly due to chemistry and not due to turbulent transport. Chemistry is rapidly adjusting the concentration of this species to the local concentrations of other reactants in the chemical scheme and the turbulent flux of the species itself is irrelevant. It is a common approach in most chemistry-transport models to use diagnostic expressions for these species, neglecting turbulent transport and assuming an instant adjustment to reaction rates and concentrations of species with longer lifetimes. Species of this category are OH and most radicals. However, chemically induced covariances may change the net production or destruction rate, and thus, for highly reactive species, the chemical equilibrium. Whether or not the segregation affects the mean concentrations, also depends on the magnitude of the inhomogeneities of the relatively stable components. For example, *Davis* [1992] estimated that the covariance of OH and isoprene depended roughly on the square of the surface emission of isoprene.

For slow reactions ($Da_c \lesssim 0.50$) the covariance of concentrations will not influence the reaction rates significantly. For these species the well-mixed assumption is justified. This is the case for ozone, PAN-like species, isoprene, and its stable degradation products such as formaldehyde, MACR, MVK, and MGLY.

In general, we find larger concentration Damköhler numbers (Da_c) in the morning than in the afternoon, with exception of OH and NO. The concentrations of the latter two species reach a maximum in the morning hour. The rates of the bimolecular reactions of OH and NO with some other species may therefore increase. This yields a smaller Da_c for OH and NO and higher Da_c for the other species in comparison with the afternoon.

For species that have moderate reaction rates ($0.5 \lesssim Da_c \lesssim 5$), turbulent transport may significantly contribute to the concentration budget. The flux Damköhler number Da_f indicates whether the turbulent transport might (potentially) be affected by higher-order chemistry terms. When $Da_f \gtrsim 0.5$ and under the condition that the fluxes are nearly stationary, then turbulent transport is significantly changed by these terms.

The turbulent flux of species with low reaction rates ($Da_c \lesssim 0.5$) can be modelled as if the gas is inert, i.e., neglecting the higher-order chemistry terms R_{wi} (equation (10)) and $R_{i\theta}$ (equation (11)). This is in both simulations the case for isoprene, ozone, H_2O_2, HNO_3, HAC, CH_3CHO and CH_3COOH. Some slowly reacting gases have moderate or high flux Damköhler numbers ($Da_f \gtrsim 0.5$), and we may find a significant chemistry effect on the flux (e.g., PAN, formaldehyde, and MGLY). However, in these cases the mean concentrations are nearly uniform throughout the BL and fluxes are very small. When these fluxes are increased owing to some external forcing (e.g., surface emissions or entrainment), chemistry effects will become insignificant owing to the large chemistry timescales.

5.2.2. Segregation effects. The chemistry scheme consists of more than 40 bimolecular reactions and according to Figure 12, many of the species involved are potentially affected by segregation effects. The chemical breakdown of isoprene can be summarized by subsequent steps of a reaction with OH forming reactive radicals, that oxidize NO to NO_2 to form stable intermediates (Figure 2). Generally, one such step decreases the number of carbon atoms by one. The bimolecular reactions were segregation effects might be relevant are therefore (1) reactions of relatively stable species such as isoprene, MACR, MVK, MGLY, and formaldehyde with the OH radical, and (2) the reaction of interme-

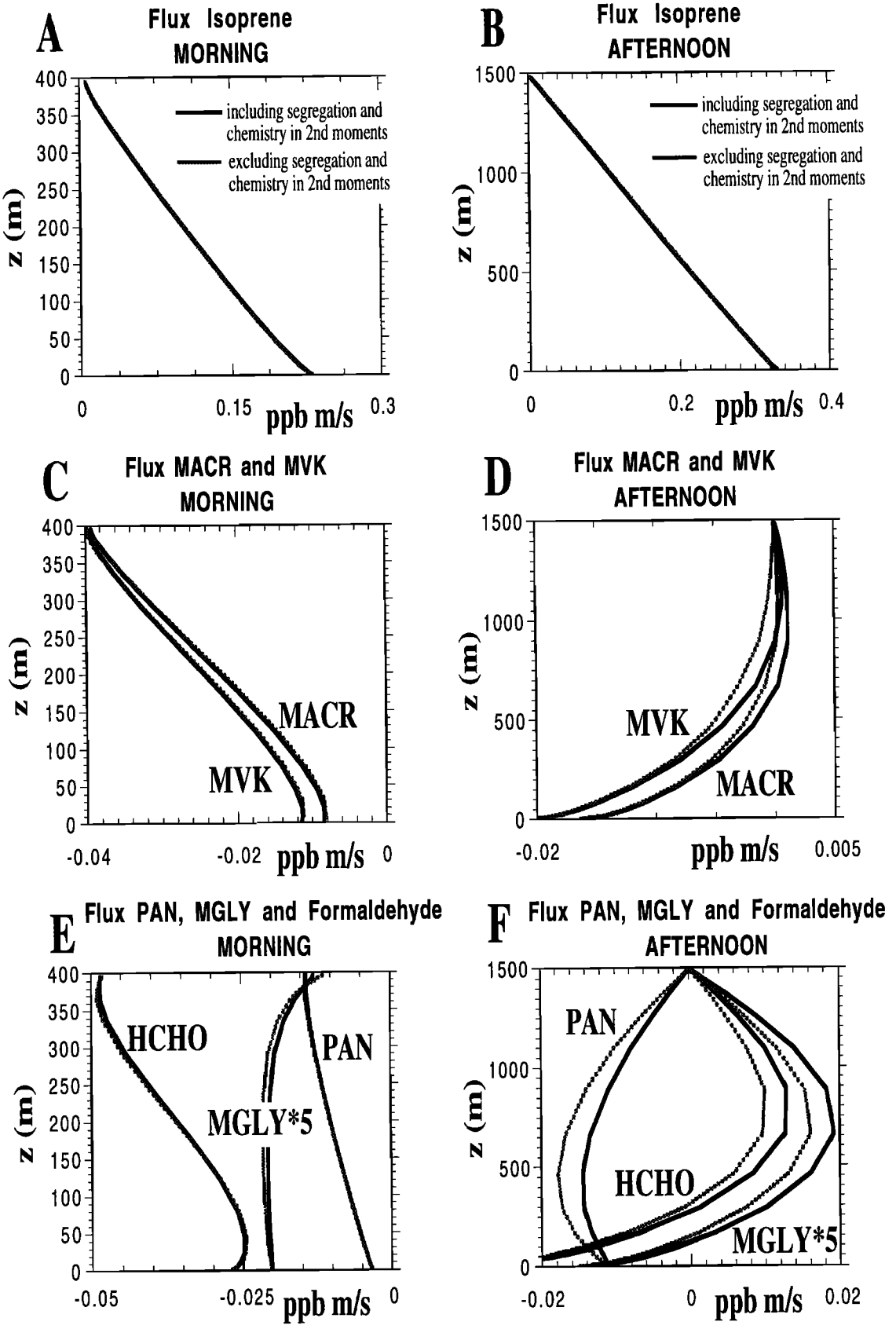

Figure 9. Flux profiles in the (left) morning and (right) afternoon of several stable species. Including (black) and excluding (grey) higher-order chemistry terms.

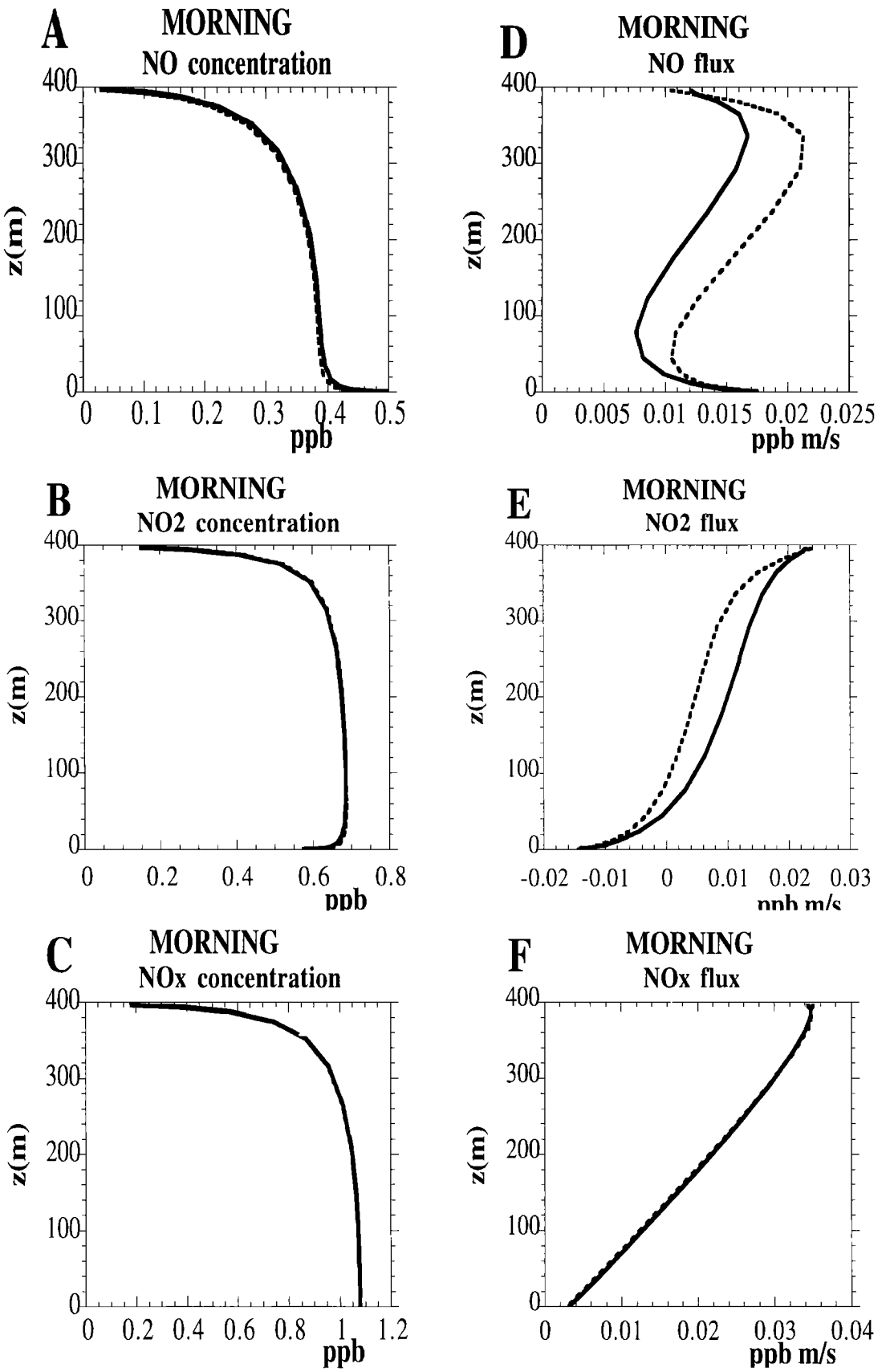

Figure 10. (Left) Concentration profiles and (right) flux profiles for (top) NO, (middle) NO_2, and (bottom) NO_x in the morning. Results of runs that included higher-order chemistry terms are plotted with solid lines; dashed lines refer to runs where these terms are neglected.

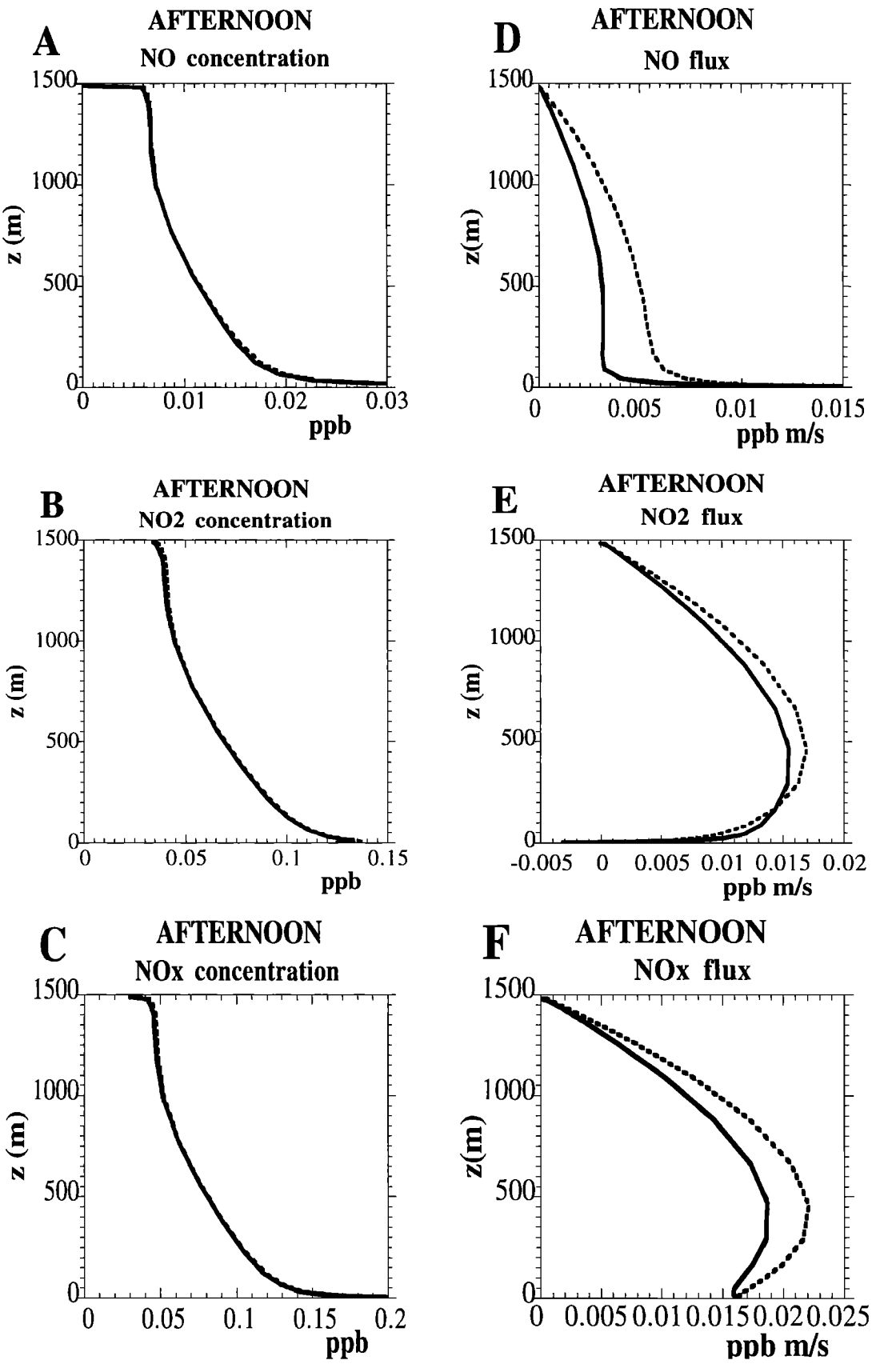

Figure 11. (Left) Concentration profiles and (right) flux profiles for (top) NO, (middle) NO_2, and (bottom) NO_x in the afternoon. Results of runs that included higher-order chemistry terms are plotted with solid lines: dashed lines refer to runs where these terms are neglected.

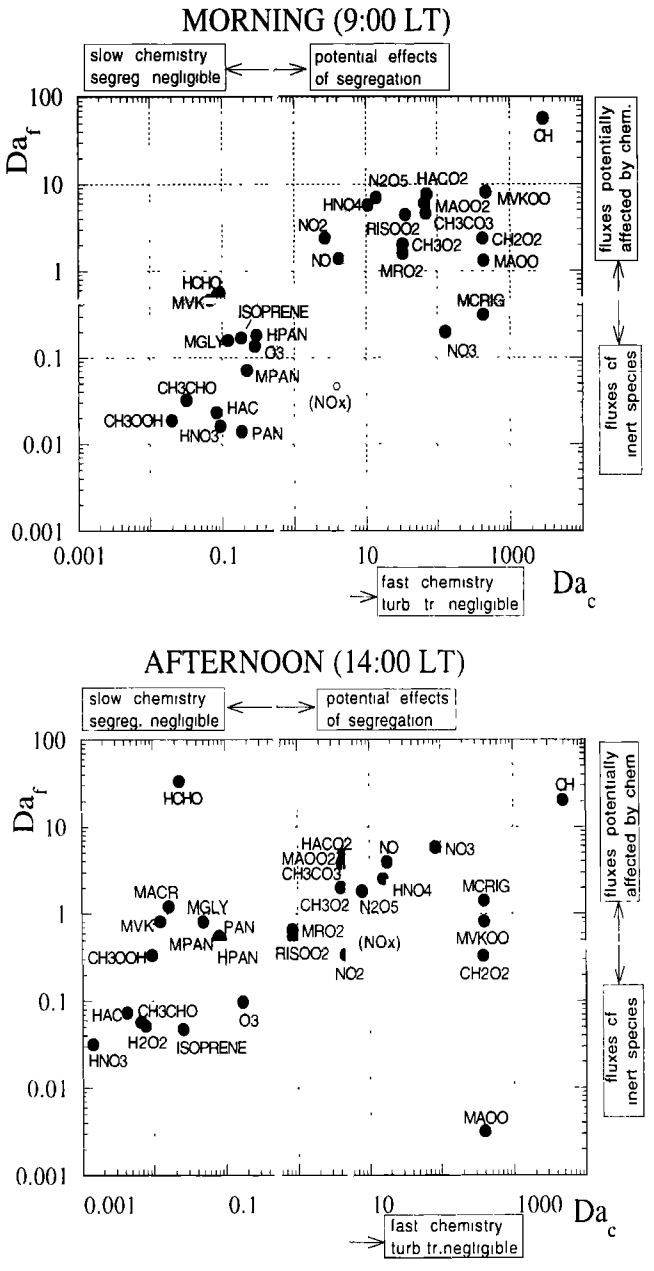

Figure 12. Bulk Damköhler numbers (Da_f) versus (Da_c) for the morning hour and for the afternoon.

diate radicals with NO. A third candidate reaction is O_3 with NO, that has been studied by many authors in previous papers on this subject. We will focus on these three types of reactions.

We have plotted concentration profiles of stable species and of some radicals in Figures 6 and 7, respectively. In Figures 6 and 7, two lines are drawn for each species: dark lines refer to model runs that included higher-order chemistry effects (segregation and chemical terms in the flux equation); light lines refer to runs where these chemistry effects have not been included.

5.2.2.1. Segregation between OH and stable species: The destruction of the reactive hydoxyl radical is caused mainly by its reaction with isoprene, and to a lesser extent by the reaction with with MVK, MACR, CO, and formaldehyde. According to their chemical lifetimes, species potentially affected ($Da_c \gtrsim 0.5$) are OH and the radicals that are formed by these reactions.

During the morning hours, large downward entrainment fluxes of the stable reaction products of isoprene (Figures 6c and 6e) cause a rapid depletion of OH in the upper part of the boundary layer (Figure 7e). Concentration fluctuations of OH and these reaction products become therefore negatively correlated due to the fact that the concentration gradients have opposite signs (see equation (3)). Figure 8a show a negative intensity of segregation throughout the boundary layer, but it significantly inhibits the mean transformation rates only in the upper 10% of the BL.

The isoprene concentration steadily increased during the morning simulation, resulting in a slightly positive entrainment flux (Figure 9a). In combination with the strong negative OH gradient caused by MACR, MVK, and other stable intermediates, this results in the positive segregation in the upper part of the BL shown in Figure 8a. The strong surface flux of isoprene causes the depletion of OH near the surface generating negatively correlated OH and isoprene concentration fluctuations. However, in the morning hours, we find a negligible segregation between OH and isoprene, except maybe very close to the top and bottom of the BL.

The afternoon situation is different in the first place because entrainment fluxes are zero, and therefore vertical gradients close to the top will be small. Close to the surface we find a negative gradient of OH due to the surface emission of NO that react with the peroxy-radicals to form OH. These reactions dominate over the depletion of OH by isoprene emitted from the surface. Despite the fact that the concentration gradients of OH and isoprene have the same sign we find a small negative I_s close to the surface (8b). This is caused by the chemistry term that dominates the covariance budget in the lowest 300 m. The bimolecular reactions of OH with MACR, MVK, and the other stable intermediates show an even smaller negative segregation close to the surface.

For both hours we did not find an impact on the mean concentration profile of OH. There might be a small impact on the profiles of other radicals, such as $RISOO_2$, but this is obscured by the segregation effects of the continuation reaction with NO, which is discussed next.

5.2.2.2. Segregation between (peroxy-)radicals and NO: The second type of reaction is the oxidation of NO by peroxy-radicals. According to Figure 12, radical concentrations, NO, and NO_2 all have $Da_c \gtrsim 0.5$, so they can potentially be affected by segregation.

Both morning and afternoon situations have a surface emission of NO and an assumed deposition flux of NO_2. In the morning the accumulated NO_x causes a positive entrainment flux of both NO and NO_2. Con-

centration and flux profiles for the morning and afternoon are depicted in Figures 10 and 11. The intensity of segregation for the reaction of NO with some radicals are given in Figure 8c and 8d for the morning and afternoon simulation, respectively.

In the morning the segregation is negative, thus inhibiting the mean transformation rate by more than 5% for most radicals, in the upper part of the BL. Since MVKOO has an almost uniform concentration profile (Figure 7c), the segregation remains close to zero throughout the BL. In the afternoon we find significant segregation effects of NO and radicals (I_s down to -0.1; Figure 8d) in the bulk of the BL. An exception again is MVKOO, with a positive I_S throughout the entire BL. It is interesting to note that in the bulk of the BL most of these profiles (i.e., those of $RISOO_2$, $MAOO_2$, and CH_3CO_3) are a result of chemistry terms in the covariance equations, so the anticorrelation is directly induced by chemistry, and not by turbulence working on the mean gradients with opposite signs.

The effect of I_s on the mean concentration is clearly seen in the peroxy-radical concentration profiles (Figure 7), with the strongest effects in the afternoon. The NO concentration profiles, however, are not affected (Figures 10a and 11a). This can be explained by the fact that any decrease or increase of effective reaction rates will mainly feedback to an increase respectively decrease of the least abundant species of the two that react, which is in this case the peroxy-radical. If we consider the chemical destruction as one chain of successive reactions, then eventually a balance of destruction and production may be reached for each species involved. The introduction of segregation in one of the bimolecular reactions in this chain will change the concentration of some of the tracers (in our case the peroxy-radicals), but if that reaction is not the rate-limiting link, it will not affect any of the transformation rates involved in the chain.

5.2.2.3. Segregation between NO and ozone: The reaction of O_3 with NO to form NO_2 takes place at a rate comparable with mixing times in the boundary layer. For O_3, $Da_c \lesssim 0.5$ in both cases, indicating that O_3 concentration profiles will not be affected by higher order chemistry terms. The intensity of segregation of both species is depicted in Figures 8c and 8d, and is small both in the morning and afternoon.

5.2.3. Chemistry effect on the flux. The model calculates turbulent fluxes by solving the flux equations including the chemistry terms (section 5.1). For fast reacting species ($Da_c \gtrsim 5$) like the radicals, the chemistry terms may dominate the flux equation ($Da_f \gtrsim 5$). However, in these cases the mean concentrations are determined by chemistry, and turbulent transport is negligible. We will therefore not discuss chemistry effects on the flux of fast reactive species.

For some slow reactive species we find a significant impact of chemistry terms on the turbulent flux ($Da_f \gtrsim 0.5$): formaldehyde, PAN, MVK, and MACR (see Figure 9). These species have nearly uniform concentration profiles (Figure 6), yielding small inert terms in the flux equation, so even small chemistry terms may dominate the flux. The mean concentration profiles are however not changed due to these terms.

We focus on the fluxes and concentrations of NO and NO_2, since they are essential in the breakdown of isoprene, and have mostly moderate reaction rates. In Figures 10 and 11 we plotted concentration and flux profiles for NO, NO_2, and NO_x, for the morning and afternoon, respectively. Solid lines refer to runs that included higher order chemistry effects; dashed lines refers to runs where these are neglected. For NO and NO_2 we find for both hours a significant impact of the higher order chemistry terms on the flux (Figure 10d, 10e, 10f, 11d, 11e, and 11f).

In the morning hours the fluxes of NO and NO_2 are mainly forced by the dilution due to the entrainment of relatively clean air from above the BL. There are no significant chemical sources and sinks of NO_x within the BL, and the NO_x flux profile is linear. The introduction of chemistry terms into the flux equation effectively causes a larger upward flux of NO_2 (+30 % in the middle of the BL) and a compensating smaller upward flux of NO. The concentration profiles, however, are not significantly affected. The decreased transport of NO to the upper part of the BL is largely offset by the segregation of NO and O_3, causing a slower production of NO_2 close to the top.

In the afternoon, fluxes of NO and NO_2 are mainly caused by the surface emission of NO and the thermal dissociation of PAN in the lower part and formation of PAN in the upper part of the BL. The reaction that involves PAN causes the increasing NO_x flux in the lower 500 m. Less NO and NO_2 is transported upward (-30% and -10%, respectively, at 500 m) when chemistry terms in the flux equation are taken into account. However, also in this simulation we do not find a significant impact on concentration profiles. The downward flux of PAN (Figure 9) is decreased with the same amount as the change of the upward NO_x flux. Since the formation of PAN is decreased by roughly 10% due to the segregation of CH_3CO_3 and NO_2 (Figure 8), it is concluded that the internal cycle of PAN formation and destruction in combination with turbulent transport in the BL has slowed down due to the introduction of higher order chemistry terms.

6. Summary and Discussion

Chemistry and air quality models typically apply conventional K theory to describe turbulent transport of reactive species. Usually, chemical transformations are also described in terms of mean concentrations only, neglecting correlated concentration fluctuations. It was suggested in previous studies (section 1 and 2) that these two approaches might give rise to errors when the chemical timescale of a species are of the same order as

the mixing timescale. Isoprene and NO have been suggested as species with such chemical lifetimes [*Davis*, 1992] that are also of interest to the background chemistry of the troposphere on a large scale. The ABLE-2A experiment provided measurements of surface fluxes of these two gases and well-documented boundary layer dynamics [*Harriss et al.*, 1988]. We used this as a realistic case to quantify the effects in a convective boundary layer. With the simple two-layer model we simulated the chemistry during several days, with prescribed boundary layer evolution. This model provided initial and boundary conditions for a one-dimensional second-order closure model including higher-order chemistry terms. Two cases were studied: the morning case with rapidly changing concentrations, relatively high OH and NO_x concentrations, and the afternoon case with much lower OH and NO_x concentrations and more slowly changing concentrations. A large range of chemical timescales were present in both cases.

We compared flux and concentration profiles of two model runs: one including the intensity of segregation I_s and chemistry terms in the flux equation and one neglecting these. The effect on the concentration profiles of the long-lived species was negligible, but profiles of the radical products were affected by 10% for some species in the afternoon, which could be attributed to segregation effects. When a short living species reacts with a stable (and therefore usually more abundant) gas, segregation effects will always feedback on the least abundant/most reactive species. In the photochemical breakdown of isoprene the concentrations of the intermediate radicals change, but they are changed such that the same amount of stable products is produced.

The OH concentration, that is mainly determined by isoprene, remained unchanged when the higher order chemistry effects were included, which may be caused by the relatively long lifetimes of isoprene during ABLE-2A.

We show that segregation can be generated by both chemistry and turbulence. Taking into account segregation effects by solving the covariance equation or by a parameterization of I_s should therefore include these higher-order chemistry effects.

The fluxes of NO and NO_2 are affected significantly by chemistry in the middle of the boundary layer in both hours that we studied. This may be relevant when, e.g., surface emissions or depositions are estimated from observed fluxes somewhere in the bulk of the boundary layer. These chemistry effects on the flux were partly compensated by the segregation of NO and O_3 (forming NO_2) in the morning and the segregation of NO_2 and CH_3CO_3 (forming PAN) in the afternoon. This seems to point at a close relation between the two higher-order chemistry effects (segregation and flux corrections) that cannot be treated separately, as is done by *Gao and Wesely* [1994].

We find significant effects of higher-order chemistry terms on the flux profiles of moderate and fast reacting species and on the mean concentration profiles of some fast reacting species. However, most global or regional scale models aim to correctly represent the distribution of mean concentrations of the longer living species, which are not so much affected by these terms.

Acknowledgments. We like to thank Maarten Krol, Laurens Ganzeveld, and two reviewers for their comments on earlier versions of this manuscript.

References

Atkinson, R., A. Lloyd, and L. Winges, An updated chemical mechanism for hydrocarbon/NO_x/SO_2 photooxidations suitable for inclusion in atmospheric simulation models, *Atmos. Environ.*, *16*, 1341–1355, 1982.

Calvert, J., and W. Stockwell, Deviations from the O_3-NO-NO_2 photostationary state in tropospheric chemistry, *Can. J. Chem.*, *61*, 983–992, 1983.

Carter, W., Condensed atmospheric photooxidation mechanisms for isoprene, *Atmos. Environ.*, *30*, 4275–4290, 1996.

Danckwerts, P., The definition and measurement of some characteristics of mixtures, *Appl. Sci. Res.*, *3*, 503–506, 1952.

Davis, K., Surface fluxes of trace gases derived from convective profiles, Ph.D. thesis, Univ. of Colorado, Boulder, 1992.

Fitzjarrald, D. R., and D. H. Lenschow, Mean concentration and flux profiles for chemically reactive species in the atmospheric surface layer, *Atmos. Environ.*, *17*, 2505–2512, 1983.

Galmarini, S., J. Vilà-Guerau de Arellano, and P. Duynkerke, The effect of micro-scale turbulent mixing on the reaction rate in a chemically reactive plume, *Atmos. Environ.*, *29*, 87–95, 1995.

Gao, W., and M. Wesely, Numerical modelling of the turbulent fluxes of chemically reactive trace gasses in the atmopheric boundary layer, *J Appl Meteorol.*, *33*, 835–847, 1994.

Gao, W., M. Wesely, and I. Lee, A numerical study of the effects of air chemistry on fluxes of NO, NO_2, and O_3 near the surface, *J. Geophys Res.*, *96*, 18,761–18,769, 1991.

Georgopoulos, P., and J. Seinfeld, Mathematical modelling of turbulent reacting plumes, I, General theory and model formulation, *Atmos. Environ.*, *20*, 1791–1807, 1986.

Gregory, G. L., E. Browell, and L. Warren, Boundary layer ozone: an airborne survey above the Amazon basin, *J. Geophys. Res.*, *93*, 1452–1468, 1988.

Guenther, A., and A. J. Hills, Eddy covariance measurements of isoprene fluxes, *J Geophys. Res.*, *103*, 13145–1315, 1998.

Hamba, F., A modified K model for chemically reactive species in the planetary boundary layer, *J. Geophys. Res.*, *98*, 5173–5182, 1993.

Harriss, R., et al., The Amazon boundary layer experiment (ABLE-2A): Dry season 1985, *J. Geophys. Res.*, *93*, 1351–1360, 1988.

Jacob, D., and S. Wofsy, Photochemistry of biogenic emissions over the Amazon forest, *J. Geophys. Res.*, *93*, 1477–1486, 1988.

Karamchandani, P., and L. K. Peters, Three-dimensional behaviour of mixing- limited chemistry in the atmosphere, *Atmos. Environ.*, *21*, 511–522, 1987.

Kirchhoff, V., Surface ozone measurements in Amazonia, *J. Geophys. Res.*, *93*, 1469–1476, 1988.

Kristensen, L., C. E. Andersen, H. E. Jorgensen, P. Kirkegaard, and K. Pilegaard, First-order chemistry

in the surface flux layer, *J. Atmos. Chem.*, *27*, 249–269, 1997.

Kuhn, M., et al., Intercomparison of the gas-phase chemistry in several chemistry and transport models, *Atmos. Environ.*, *32*, 693–709, 1998.

Martin, C., D. Fitzjarrald, M. Garstang, A. Oliveira, S. Greco, and E. Browell, Structure and growth of the mixing layer over the Amazonian rain forest, *J. Geophys. Res.*, *93*, 1361–1375, 1988.

Kaplan, W., S. Wofsy, M. Keller, and J. daCosta, Emission of NO and deposition of O_3 in a tropical forest system, *J. Geophys. Res.*, *93*, 1389–1395, 1988.

Nappo, C., and H. van Dop, A boundary layer parameterization for global dispersion models, *J. Geophys. Res.*, *99*, 10527–10534, 1994.

Petersen, A., and A. Holtslag, A first-order closure for covariances and fluxes of reactive species in the convective boundary layer, *J. Appl. Meteorol.*, (in press), 1999.

Schumann, U., Large-eddy simulation of turbulent diffusion with chemical reactions in the convective boundary layer, *Atmos. Environ.*, *23*, 1713–1727, 1989.

Trainer, M., E. Hsie, S. McKeen, R. Tallamraju, D. Parrish, F. Fehsenfeld, and S. Liu, Impact of natural hydrocarbons on hydroxyl and peroxy radicals at a remote site, *J. Geophys. Res.*, *92*, 11,879–11,894, 1987.

Verver, G. H. L., Comment on "A modified K model for chemically reactive species in the planetary boundary layer", by Fujihiro Hamba, *J. Geophys. Res.*, *99*, 19,021–19,023, 1994.

Verver, G. H. L., H. van Dop, and A A. M. Holtslag, Turbulent mixing of reactive gases in the convective boundary layer, *Boundary Layer Meteorol.*, *85*, 197–222, 1997.

Vilà-Guerau de Arellano, J., and P. G. Duynkerke, Influence of chemistry on the flux-gradient relationships for the NO-O_3-NO_2 system, *Boundary Layer Meteorol.*, *61*, 375–387, 1992.

Vilà-Guerau de Arellano, J., and J. Lelieveld, Chemistry in the atmospheric boundary layer, in *Clear and Cloudy Boundary Layers*, edited by A. Holtslag and P. G. Duynkerke, p. 360, Netherland Academy of Arts and Sciences, Amsterdam, 1998.

Vilà-Guerau de Arellano, J., A. Talmin, and P. Builtjes, A chemically reactive plume model for the NO-NO_2-O_3 system, *Atmos. Environ., Part A*, *24*, 2237–2246, 1990.

Wesely, M., Parameterization of surface resistances to gaseous dry deposition in regional scale numerical models, *Atmos. Environ.*, *6*, 1293–1304, 1989.

Zimmerman, P., J. Greenberg, and C. Westberg, Measurements of atmospheric hydrocarbons and biogenic emission fluxes in the Amazon boundary layer, *J. Geophys. Res.*, *93*, 1407–1416, 1988.

A. A. M. Holtslag, Meteorology and Air Quality Section, Wageningen University, Wageningen, The Netherlands.

H. van Dop, Istitute for Marine and Atmospheric Research, Utrecht University, Utrecht, The Netherlands.

G. H. L. Verver, Royal Netherlands Meteorological Institute, De Bilt AE 3730, The Netherlands. (e-mail: verver@knmi.nl)

(Received January 25, 1999; revised September 8, 1996; accepted September 12, 1999.)